Fire Response of a Carbon Epoxy Composite: Comparison of the Degradation Provided with Kerosene or Propane Flames

Chazelle T., Perrier A., Schuhler E., Cabot G., Coppalle A.*

Normandy University, INSA Rouen, CORIA St. Etienne du Rouvray, France
**Corresponding author's email: alexis.coppalle@coria.fr*

ABSTRACT

In the aeronautics, composite materials are widely used. An important issue is that they may be exposed to a flame, during a malfunction of the engines or after a crash. This work is a comparative study, at laboratory scales, of the degradation of carbon epoxy composites with impinging jets of kerosene and propane flames. The propane and kerosene burners have been developed to allow the exposition of small composite samples, of few cm sizes, to heat fluxes greater than 110 kW/m^2. The sample holders were designed to carry out measurement of the mass loss rate and IR temperatures at the rear face during tests. For the two flame tests, the mass loss is nearly complete after 300 s, the resin is almost degraded throughout the sample depth, leaving the fibers naked on the front face, and a small amount of degraded resin on the rear face. However the speed of the degradation is slower with the kerosene flame, with a maximum temperature value reached at the rear face lower than for the propane flame. This is explained by the presence of high amounts of soot in the kerosene flame, while they are nearly non-existent in the propane flame. The high soot content in the kerosene flame induces the built-up of a black carbon layer on the front face, which may reduce the heat transfer between the impinging flame and the sample face.

KEYWORDS: Composites, fire reaction, propane flame, kerosene flame.

NTRODUCTION

In the aeronautics, composite materials are now widely used. Unfortunately under some circumstances, as a malfunction of the engines or after a crash, they may be exposed to a flame. Then the composite is degraded and it losses its mechanical performances. In order to test the fire reaction of the materials, there are several standard tests specific to aeronautical applications [1], in particular some of them use propane or kerosene impinging flames [2-3]. In research at laboratory scales, most of tests are done with a cone calorimeter to apply a radiative flux on the sample [4-5]. Up to now, there are much less studies which have used a flame to induce thermal stress on the material [6-8]. The mains advantages of a flame exposure is that heat fluxes greater than 100 kW/m^2 can be easily reached and a direct flame impact is a more realistic stress for a lot of fire scenarios.

An impinging jet flame induces both convective and radiative fluxes, with different contribution depending on the nature of the fuel. In the case of a non-sooting flame, like the one produced by a burner supplied in stoichiometric conditions, the convective flux is important. With a kerosene flame, the soot production is higher, which increases the contribution of the radiative flux. Another important issue is the soot deposition on the sample, which may be high with kerosene flames, and it can change the heat transfer inside the sample.

The main aim of this work is to compare, at laboratory scales, the degradation of a carbon epoxy composite under the thermal stress provided by a kerosene or propane flame. The burner designs and the flames properties are presented. Details are given on the sample holders and measurement

Proceedings of the Ninth International Seminar on Fire and Explosion Hazards (ISFEH9), pp. 950-958
Edited by Snegirev A., Liu N.A., Tamanini F., Bradley D., Molkov V., and Chaumeix N.
Published by Saint-Petersburg Polytechnic University Press
ISBN: 978-5-7422-6498-9 DOI: 10.18720/spbpu/2/k19-17

systems. The results of mass loss rates and IR temperatures at the rear face, obtained during several tests are shown and discussed.

BURNERS AND FLAME PROPERTIES

The propane burner is similar to the one used in [8], and its design is schematized below on Fig. 1 a. The propane combustion is produced in a small chamber in stoichiometric proportions, and the combustion products are injected inside a long flame-tube (50cm long and 3.5 cm diameter), thus providing at the exit an homogeneous flux of hot gases at the surface of the composite sample. Fig. 1 b shows a picture of the flame impinging one sample during a test. A screen put just above the sample holder can also be seen on the picture, and it avoids the hot gas recirculation on the rear face of the sample. The sample holder itself is placed 17 mm above the burner exit. The design of the sample holder is provided in Fig. 2. An aperture of 45mm diameter is made on both sides of the holder, on the front size to delimit the surface exposed to the flame impact and on the back side to enable the IR temperature measurement. The samples are square shaped with size of 50 mm.

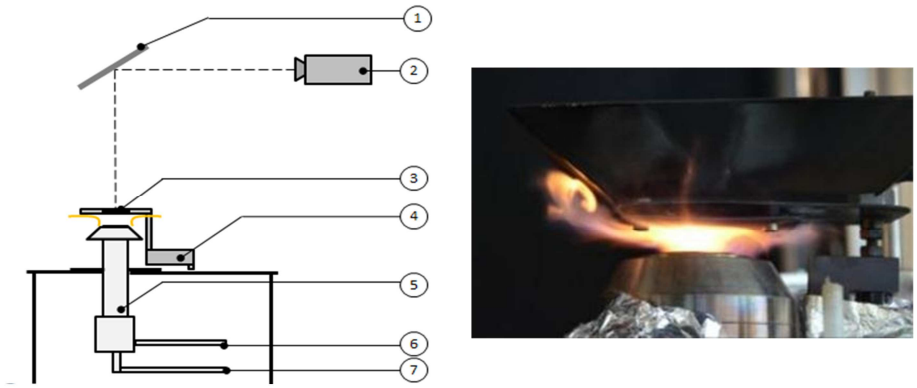

(a) (b)

Fig. 1. (a) Schematic view of the propane burner and the associated measurement setup (1 – mirror, 2 – infrared camera, 3 – sample holder, 4 – load cell, 5 – burner, 6 – air inlet, 7 – propane inlet); (b) picture of the flame impinging one sample during a test

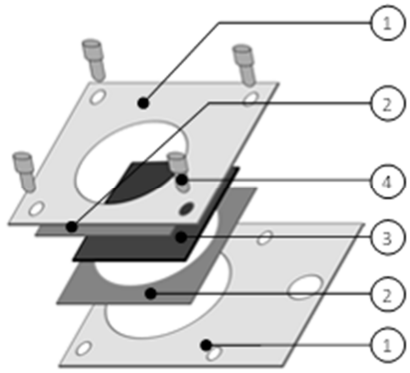

Fig. 2. Schematic of the sample holder for the propane flame case.
1 – sample holder, 2 – insulation sheet, 3 – sample, 4 - screw

The sample degradation by the kerosene flame is based on the same principle. The test bench used for this work is shown in Fig. 3 a. In it, a fuel domestic burner, fed with kerosene and with an air to

combustible ratio equals 0.85 of the stoichiometric value, generates a turbulent jet flame. This lower value of the air to combustible ratio for the kerosene burner has been required to obtain the same heat flux and temperatures as with the propane burner A tube is put around the exit of the burner, and it is ended by a flame-tube of 30 cm long and 5 cm diameter (Fig. 3 b). The sample holder is placed 50 mm from the flame-tube exit. A picture of the sample holder for the kerosene tests is provided in Fig. 4. An aperture of 50mm diameter is made alike on both sides of the holder, for delimiting the surface exposed to the flame and to enable the IR temperature measurement on the rear face. The samples are square shaped with a size of 100mm.

Before each test and for both flames, heat flux and flame temperature measurements are carried out with the sample holder removed and at the same location in the free flame. The heat flux is measured using a water cooled heat flux sensor (Captec manufacturer) inserted into a movable steel plate, as shown for example in Fig. 5 for the kerosene flame. Likewise, the temperature is measured using a movable row of 5 type K thermocouples, the spacing between each thermocouple being 7 mm. After the burner ignition, a period of ten minutes is necessary in order to reach steady conditions in temperature and flux. For the propane and kerosene flames, respectively, the mean temperature on the axis is 1110 °C and 1110°C, and the heat flux is 106 kW/m^2 and 116 kW/m^2.

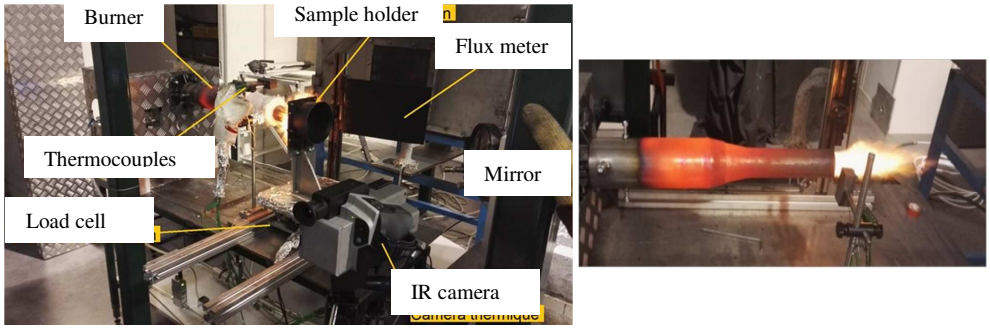

Fig. 3. (a) The kerosene burner and the measurement setup, (b) picture of the flame exiting of the flame-tube (without insulation).

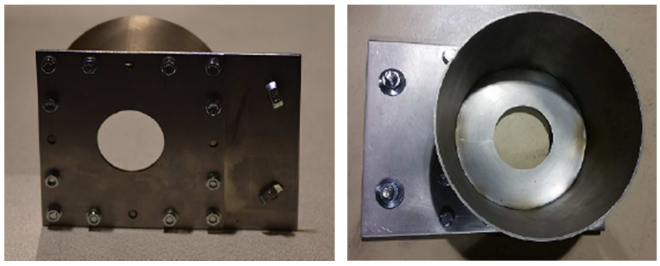

(a) (b)

Fig. 4. Pictures of the sample holder for the kerosene flame case, (a) front face (b) rear face.

MASS LOSS AND IR TEMPERATURE MEASUREMENTS DURING THE TESTS

For the tests with the propane flame, the mass is monitored using a precision load cell, based on resistive foil technology (VPG transducers manufacturer), to which is attached the sample holder. For the tests with the kerosene flame, the sample holder is too heavy to use the same system. So it has been used a weigh scale on which the sample holder has been placed, as seen on Fig. 3 a. The precision of both systems is 0.01g.

The temperature of the rear face of the samples has been observed using an IR camera. The propane and kerosene benches are equipped with a mirror located far away from the sample holder and an infrared camera model ThermaCam PM595 (Fig. 1 a and Fig. 3 a). With this layout, the camera is looking at right angle to the burner axis and it is outside the hot gas flow. The major drawback of the IR measurement method is ignorance, during tests, of the degraded surface emissivity. Therefore we assumed the emissivity to be constant and equal to 0.9, as measured on carbon fibers by Balat-Pichelin et al. [9]. It is also a common value used in the literature for char [10]. However the method allows a temperature measurement of the whole sample surface and so to analyze the temperature homogeneity on the rear surface.

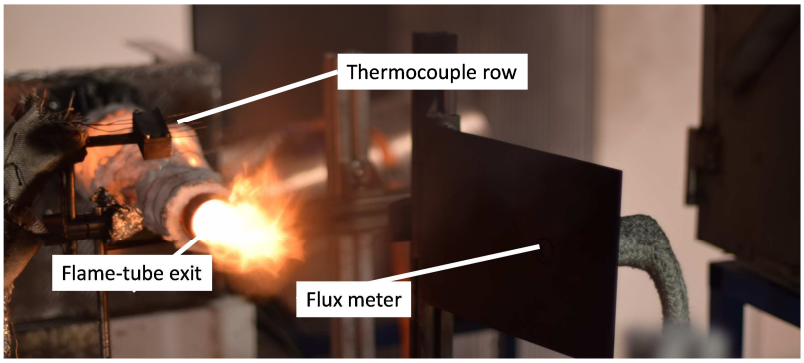

Fig. 5. Picture showing the free kerosene jet flame exiting the flame-tube, the thermocouple row and the flux meter inserted into a steel plate.

COMPOSITE MATERIAL

The samples studied in this work are cut from a 2 mm thick plate, with 50x50 mm² and 100x100 mm² sizes for the propane and kerosene flame respectively. The plate is epoxy-based reinforced with carbon fibers, this composite can be considered as a reference since it has been common CFRP material used in aeronautic structural parts for more than 30 years. The stacking sequence of carbon fiber (T300 3K) is 5-harness satin weave embedded in the polymer matrix. The mass fraction of fiber is 74%. The degradation onset temperature T_d is 320°C and the peak of mass loss rate occurs at temperature T_p equal to 390°C, as shown in Fig. 6.

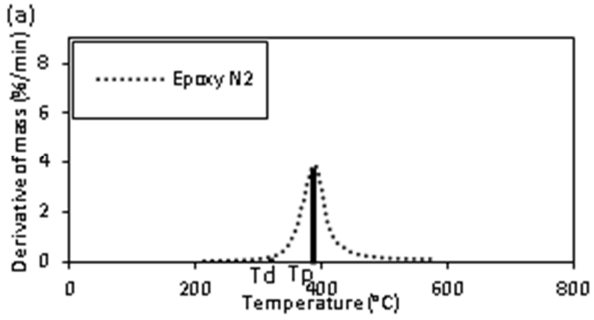

Fig. 6. DTG results for the C/epoxy composite materials in N_2 [8].

RESULTS AND DISCUSSIONS

The samples have been exposed during 300 s to the flame and then the sample holder is removed quickly. For each flame, three tests have been carried out in order to check the reproducibility of the experimental setup as a whole.

Sample appearance after the test

Fig. 7 shows the C/epoxy appearance of one sample, after 300s exposition to the propane flame. On the front side, there is no more matrix residue, the fibers are naked and the surface is slightly curved. A slight deposit has been observed on the front face. On the other side, not exposed to the flame, there is still a small amount of resin residue between the fibers. The back surface has remained more or less flat.

On Fig. 8 is shown the appearance of another sample, after 300s exposition to the kerosene flame. The front side aspect is different, compared to the one obtained with the propane flame. An significant soot layer has been deposed and the surface is not curved. On the other hand, the back face looks like more or less the same as the one observed with the propane flame.

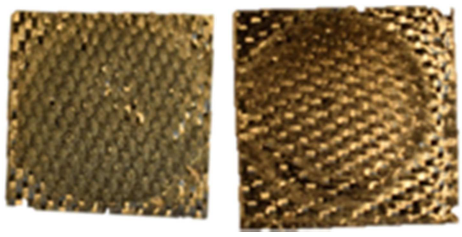

(a) (b)

Fig. 7. View of the C/epoxy sample, after 300s exposition to the propane flame, of the back face (a) and of the front face (b).

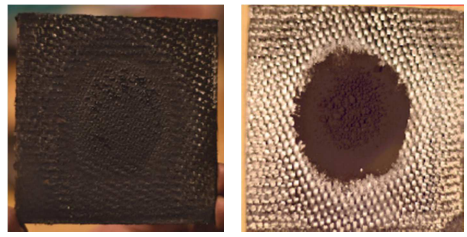

(a) (b)

Fig. 8. View of the C/epoxy sample, after 300s exposition to the kerosene flame, of the back face (a) and of the front face (b).

Mass loss

The mass loss of the C/epoxy samples exposed to the propane or kerosene flames is given in Fig. 9. First of all, one can see that the reproducibility of the measurements is good for the two experimental setups. However, there are important differences in the fire response of the composite. For the kerosene flame, the mass loss is much slower at the beginning and reaches, at 300 s, values that are lower than in the propane flame tests. For this last one, all the mass loss occurs during the first 100 s of the tests. While for the kerosene flame, the mass loss seems not finished at 300 s.

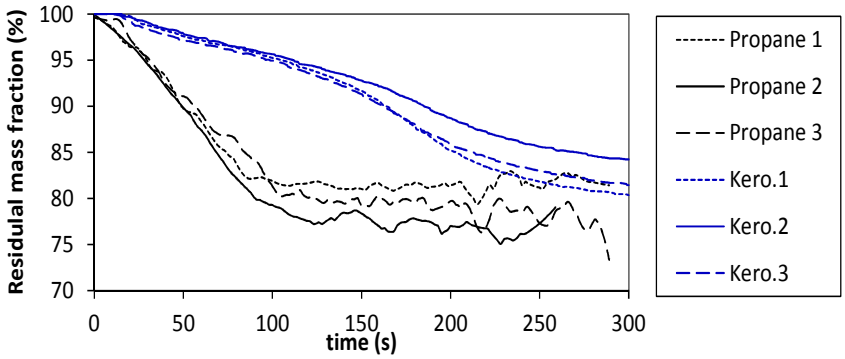

Fig. 9. Mass loss fraction of the C/epoxy samples, exposed to the propane or kerosene flames.

Table 1. Mass before and after the three kerosene tests. All mass in [g]

	Kero 1	Kero 2	Kero 3
Sample mass before the test	29.94	27.78	29.08
Sample holder mass before the test {A}	1879.68	1878.74	1880.61
Sample holder mass with the soot deposit {B}	1873.41	1874.17	1874.89
Sample holder mass without the soot deposit {C}	1873.22	1874.05	1874.78
Total sample mass loss {A-B}	6.27	4.57	5.72
Soot mass deposit {B-C}	0.19	0.12	0.11
Soot mass deposit	3.0%	2.6%	1.9%

Before and after each test, it is easy to measure the mass of the sample and its holder. Table 1 gives these values for the three kerosene tests. The differences between the sample holder mass before {A} and after {B} the tests provide the total sample mass losses. One could suspect that these values may be under estimated because of soot deposit. The mass difference between the sample holder with the soot deposit on the entire surface {B} and without {C} is equal or less than 3%. The exact value of deposited soot mass on the exposed surface of the sample is thus lesser, due to the ratio of the exposed surface exposed to sample holder. So the soot deposit occurs however it represents a small mass compared to the total mass loss.

Temperature at the back face

Figure 10 presents, for test 'kero 1', the back face temperature, as measured by the IR camera at 150s. No temperature inhomogeneity is observed on the rear face zone delimited by the aperture of 5cm made in the sample holder. This suggest that most part of the thermal flux applied on the corresponding zone on the front of the sample holder, and also delimited by an aperture of 5cm, is transmitted through the depth of sample, with a low radial flux. For all the other tests with kerosene or propane, pictures and similar temperature homogeneities, as the ones shown on Fig. 1, have been observed.

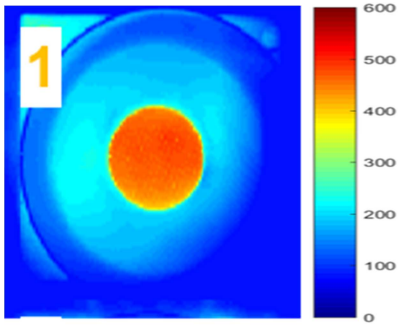

Fig. 10. Back face temperature for test 'kero 1' measured by the IR camera at 150s.

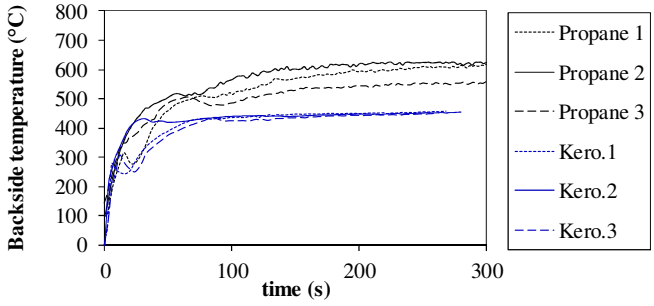

Fig. 11 Back side temperatures at the center of the samples and reported as a function of the exposure time

Backside temperatures measured at the center of the samples and with the infrared camera are reported on Fig. 11 as a function of the exposure time.

During the first 20 s, the temperature increases quickly and in the same way for both flame fluxes, indicating a strong thermal conduction through the sample thickness. The heating rate at the back

face approaches 750 K/mn. During this stage, the temperature gradient between the front-face and the back-face is very high, which must lead to high thermally-induced mechanical strains into the material, resulting in micro-cracks formation within the matrix and debonding between plies, as it has been shown in the previous work [8].

At the end of this first period, the temperatures lie between 250–300 °C. This temperature range corresponds to the thermal decomposition of the matrix as shown in Fig. 6. In the second period, the temperature increase slows down. For some tests (propane 1, Kero 1 and 3), the values drop significantly. This observation is associated with the occurrence of thermally induced cracks within the sample [8, 11-12]. It is assumed that the cracks act as a thermal barrier and therefore affect the thermal conduction through the sample. It is important to note that this phenomenon does not occur automatically since it is not observed for half of the tests. Another important question, that would be interesting to answer, is to determine if this cracks occur slowly and later for these tests. One can observe that, even when the cracks do not occur at the beginning, these samples reach the same final temperature as the others.

This final temperature at the back face is lower for tests with kerosene, the difference is quite significant (>100°C). This can be explained by the soot deposit on the front face, which is non negligible for the kerosene flame. At the beginning of the tests, it seems to be low, since no strong differences of the temperature are observed on Fig. 11 during first period up to 20 s. After this period, it becomes bigger. It may act as a thermal barrier, reducing the heat transfer inside the sample, and thus the temperature increase is slowed down which delays also the degradation of the resin. This is observed on the mass loss curves on Fig. 9, which show that the mass loss rate is lower for the kerosene flame from the first moments of the tests. In order to check this assumption, the thermal resistance of a soot layer must be estimated. In a steady-state regime, the temperature variation inside the soot deposit is given by the Fourier law:

$$\Phi = k_{eff} \frac{dT}{dx}, \tag{1}$$

where Φ is the heat flux at the exposed surface, x is the coordinate along the depth and k_{eff} is the effective heat conductivity of the soot layer. At the end of the test, the back face temperature does not vary any more with time, so the assumption of a steady-state heat transfer can be assumed. So the temperature gap inside the soot layer is given by the relation

$$\Delta T = \Phi \frac{l}{k_{eff}}, \tag{2}$$

l being the thickness of the layer. The effective conductivity of the soot deposit layer is a function of the porosity ε of the porous medium, which is defined by $\varepsilon = V_g / V$, where V_g is the volume of gas in the porous medium and V its total volume. Tavman [13] has made an inventory of existing relationships to express the effective thermal conductivities of porous materials. As part of our study, we take the minimum and maximum values given by Tavman [13]:

$$\frac{1}{k_{eff,\perp}} = \frac{\varepsilon}{k_g} + \frac{1-\varepsilon}{k_p} \tag{3}$$

for the series mixing case, and

$$k_{eff,\parallel} = \varepsilon k_g + (1-\varepsilon) k_p \tag{4}$$

for the parallel mixing case. In Eqs. (3) and (4), k_g and k_p are the heat conductivity of the gas and of the particle matter respectively. In order to apply Eq. (2), the soot layer depth is supposed to be equal to 0.5 mm, and different extreme cases have been considered. They are given in Table 2. The heat conductivity of the gas inside the soot layer has been taken equal to that one of air at 600 K, 0.046 W/(m·K), and those of the soot particle matter equal to the one of graphite at ambient temperature, 4.2 W/(m·K).

It is hard to decide which case, series or parallel, is representative of the soot material. On the other side, the exact value of the porosity is certainly between the two extreme ones used in table 2. However some calculated ΔT values in this table may be real and close to difference observed between the kerosene and propane flames, at the end of the test. This crude estimation of the temperature gap shows that the soot deposit layer may act as a thermal barrier, reducing the heat transfer inside the sample. Further studies are necessary to determine more accurately the porosity and depth of the soot deposit, and to perform calculation in an unsteady regime, in order to explain the differences of temperature variations observed between the propane and kerosene flames.

Table 2. For the soot deposit layer: values of the effective heat conductivity and the corresponding temperature gap, considering two different porosity values and using the series or parallel mixing laws

Porosity	$\varepsilon = 0.1$	$\varepsilon = 0.9$
$k_{eff,\perp}$, W/(m·K)	0.42	0.052
ΔT, K[a]	130	1057
$k_{eff,\parallel}$, W/(m·K)	3.78	0.462
ΔT, K[a]	14	119

[a] $\Phi = 110$ kW/m^2.

CONCLUSION

A comparative study, at laboratory scales, of the degradation of carbon epoxy composites with impinging jets of kerosene and propane flames has been carried out. The sample holders were designed to carry out measurement of the mass loss rate and IR temperatures at the rear face during tests. Measurements obtained with three different tests and with the same conditions show that the reproducibility of the two test benches is good, and such systems are well designed to analyze the composite degradation at laboratory scales.

Under a flux of 110 kW/m^2, the mass loss is nearly complete after 300 s for the two cases, the resin is almost degraded throughout the sample depth, leaving the fibers naked on the front face, and a small amount of degraded resin on the rear. However, under the same flux, the speed of the degradation is slower with the kerosene flame, the maximum temperature value reached at the rear face is about 150 °C lower than the one obtained with the propane flame. This is explained by the presence of high amounts of soots in the kerosene flame. This high soot content in the kerosene flame induces the built-up of a black carbon layer on the front face. A rough estimation of the thermal resistance of this soot layer has shown that it may reduce the heat transfer between the impinging flame and the sample face.

Further studies are necessary to determine more accurately the porosity and depth of the soot deposit, and to perform more accurate calculations of the thermal resistance of the soot layer on the front face. Comparison with large scale test results is also important and it will be done in future.

REFERENCES

[1] A.P. Mouritz, A.G. Gibson. Fire Tests for Composites. In: Fire Properties of Polymer Composite Materials. Solid Mechanics and its Applications Vol. 143, 2006, Springer, Dordrecht.

[2] ISO2685:1998(E). Aircraft-environment test procedures for airborne equipment – resistance to fire in designated fire zones.

[3] FAR25.856(b):2003. Title 14 code of Federal – test methods to determine the burnthrough resistance of thermal/acoustic insulation materials (Appendix F, Part VII).

[4] S.I. Stoliarov, S. Crowley. R.E. Lyon, G.T. Linteris. Prediction of the burning rates of non-charring polymers. Combust. Flame 156 (2009) 1068-1083.

[5] N. Grange, K. Chetehouna, N. Gascoin, A. Coppalle, I. Reynaud, S. One-dimensional pyrolysis of carbon based composite materials using FireFOAM, Fire Saf. J. 97 (2018) 66–75.

[6] A.G. Gibson, W.N.B. Wan-Jusoh, G. Kotsikos, A propane burner test for passive fire protection (PFP) formulations containing added halloysite, carbon nanotubes and graphene, Polym. Degrad. Stab. 148 (2018) 86–94.

[7] P. Tranchard et al. Fire behaviour of carbon fibre epoxy composite for aircraft: Novel test bench and experimental study, J. Fire Sci. (2015) 1–20.

[8] E. Schuhler, A. Coppalle, B. Vieille, J. Yon, Y. Carpier, Behaviour of aeronautical polymer composite to flame: A comparative study of thermoset- and thermoplastic-based laminate, Polym. Degrad. Stab. 152 (2018) 105-115.

[9] M. Balat-Pichelin, J.F. Robert, J.L. Sans, Emissivity measurements on carbon–carbon composites at high temperature under high vacuum, Appl. Surf. Sci. 253 (2006) 778-783.

[10] J.B. Henderson, T.E. Wiecek, A Mathematical Model to Predict the Thermal Response of Decomposing, Expanding Polymer Composites. J. Comp. Mat. 21 (1987) 373-393.

[11] A.P. Mouritz, A.G. Gibson, Fire Properties of Polymer Composite Materials. Solid Mechanics and its Applications Vol. 143, 2006, Springer, Dordrecht.

[12] G. Leplat, C. Huchette, V. Biasi, Thermal and damage analysis of laser-induced decomposition within carbon/epoxy composite. J. Fire Sci. 34 (2016) 361-384.

[13] I.H. Tavman, Effective thermal conductivity of granular porous materials, Int. Comm. Heat Mass Transfer 23 (1996) 169-176.

[14] W.C. Hinds, Aerosol technology: properties, behaviour, and measurement of airborne particles (2nd ed.), Wiley Interscience, New York, 1999.